Electronic Supplementary Material (ESI) for Materials Chemistry Frontiers.

Supporting Information

Self-assembled Organic Nonlinear Optical Crystals Based on Pyridine Derived Fluorenone

Yongshen Zheng, Puxin Cheng, Xiaodong Qian, Junjie Guan, Rongchao Shi, Mingyang Xin, Jialiang Xu* and Xian-He Bu

School of Materials Science and Engineering, Smart Sensing Interdisciplinary Science Center, Collaborative Innovation Center of Chemical Science and Engineering, Nankai University, Tongyan Road 38, Tianjin 300350, P. R. China

*E-mail: jialiang.xu@nankai.edu.cn

Experimental Section

1. Materials and Methods

All the chemicals and solvents are of reagent grade commercially purchased. Powder X-ray diffraction (PXRD) patterns and variable-temperature powder X-ray diffraction (VT-PXRD) patterns were collected by a Rigaku MiniFlex600. The UV-vis absorbance spectra were obtained on a UV-vis spectrophotometer (UV 2600). The photoluminescence spectra were obtained on a fluorescence spectrophotometer (F-7000). Single crystal data were collected on a Rigaku XtalAB PRO MM007 DW diffractometer with Cu Kα radiation (λ = 1.5418 Å) or Mo Kα radiation (λ = 0.71073 Å). Thermogravimetric analyses (TGA) measurements were carried out under air atmosphere in a TA instruments Q50 thermal analyzer, with a constant heating rate of 10 °C/min. Differential scanning calorimetry (DSC) data were obtained on a TA DSC-25 instrument with cooling and heating rates both of 5 °C/min. ^{1}H and ^{13}C NMR spectra were obtained on a Bruker 400 MHz. The mass spectrometry (MS) was obtained on a Shimadzu LCMS-IT-TOF. The elemental analysis was characterized by CHONS elemental analyzer (Vario EL cube). The time-resolved PL decay curves and PLQYs were collected by spectrofluorometer (Edinburgh FS-C05) at RT. NLO measurements were performed using a home-built set-up in the reflection geometry.[1] All the DFT/TD-DFT calculations were carried out in the E.01 version of Gaussian09.[2] The B3LYP functional and 6-31G++ basis were adopted to obtain the HOMO and LUMO wavefunctions and the molecular dipole moments of 3-DPyFO and 4-DPyFO S_0 state. We have selected B3LYP/6-31G+(d) basis to calculate the transition density of states from S_0 to different excited states. The visualizations were displayed by VMD software.[3] The Hirshfeld surface calculations were implemented in CrystalExplorer.[4] The overall permanent dipole moments in a unit cell have been performed in the first-principles code Vienna ab initio simulation package (VASP).[5]

2. Synthesis

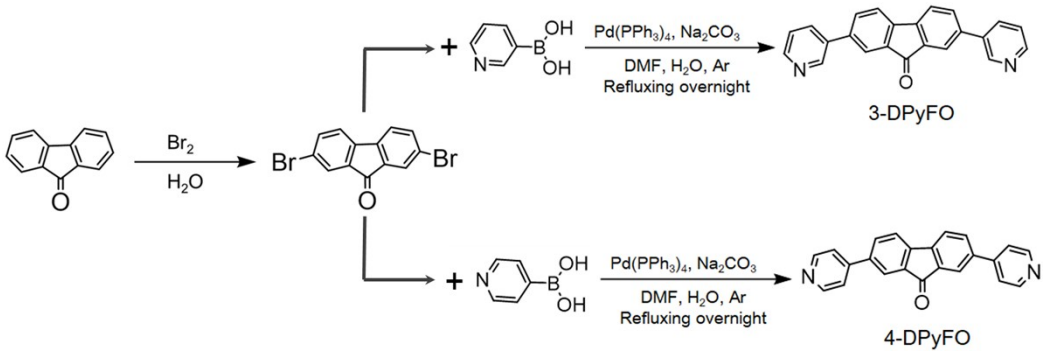

Scheme S1. Synthesis route of the target compound 3-DPyFO and 4-DPyFO.

2.1 Preparation of 2,7-dibromo-9-fluorenone: The synthetic route to the precursors 2,7-dibromo-9-fluorenone was shown in Scheme S1.[6] Pure Br_2 (7.15 mL, 138.7 mmol) was added to the aqueous suspension (70 mL) of 9-fluorenone (5.0 g, 27.7 mmol)

drop by drop at 0 °C, and then the system was stirred at 80 °C for 10 hours. After cooling to room temperature, 100 mL of H_2O was added to the reaction system, then an appropriate amount of saturated Na_2SO_3 solution was added. The yellow precursor 2,7-dibromo-9-fluorenone (9.07 g, 27.15 mmol) was obtained by filtration and washing with water several times. The crude product was then purified by recrystallization in n-hexane to give the yellow powder. Yield: ~95%. ^{1}H-NMR (400 MHz, $CDCl_3$, δ): 7.78 (s, 2H, Ar H), 7.63 (d, 2H, Ar H), 7.39 (d, 2H, Ar H). ^{13}C-NMR (101 MHz, $CDCl_3$, δ): 190.94, 142.27, 137.49, 135.28, 127.86, 123.34, 121.86.

2.2 Synthesis of 3-DPyFO: Under an argon atmosphere, $Pd(PPh_3)_4$ (233 mg, 0.2 mmol) was added to a stirred mixture of precursors 2,7-dibromo-9-fluorenone (1.36 g, 4.0 mmol) , 3-pyridineboronic acid (989.0 mg, 8.0 mmol) and Na_2CO_3 (4.26 g, 40.0 mmol) in 50.0 mL of *N,N*-dimethylformamide (DMF) and 5.0 mL of water. The reaction mixture was refluxed at 150 ℃ for 24h. After cooling and removing most of the solvent in vacuum, the mixture was dissolved in 200 mL of CH_2Cl_2, and the organic phase was washed with saturated NaCl aqueous solution several times and dried over Na_2SO_4. The crude product was purified by column chromatography (silicagel, ethyl acetate) to give yellow powder (884 mg, 2.64 mmol). Yield: ~66%. ^{1}H-NMR (400 MHz, $CDCl_3$, δ): 8.88 (d, 2H, Ar H), 8.64 (dd, 2H, Ar H), 7.90 (m, 4H, Ar H), 7.73 (dd, 2H, Ar H), 7.67 (d, 2H, Ar H), 7.40 (q, 2H, Ar H). ^{13}C-NMR (101 MHz, $CDCl_3$, δ): 191.98, 148.00, 146.77, 142.53, 138.03, 134.36, 134.28, 133.17, 132.44, 122.76, 122.08, 120.28. MS (ESI+) m/z: [M+H]+ Calcd for C23H14N2O, 334.36; found 335.28. Anal. Calcd for C23H14N2O: C 82.64, H 4.19, N 8.38, O 4.79; found: C 82.46, H 4.19, N 8.46, O 4.89.

2.3 Synthesis of 4-DPyFO: Under an argon atmosphere, $Pd(PPh_3)_4$ (233 mg, 0.2 mmol) was added to a stirred mixture of precursors 2,7-dibromo-9-fluorenone (1.36 g, 4.0 mmol), 4-pyridineboronic acid (989.0 mg, 8.0 mmol) and Na_2CO_3 (4.26 g, 40.0 mmol) in 50.0 mL of DMF and 5.0 mL of water. The reaction mixture was refluxed at 150 ℃ for 24h. After cooling and removing most of the solvent in vacuum, the mixture was dissolved in 200 mL of CH_2Cl_2, and the organic phase was washed with saturated NaCl aqueous several times and dried over Na_2SO_4. The crude product was purified by column chromatography (silicagel, ethyl acetate) to give yellow powder (965 mg, 2.85 mmol). Yield: ~71%. ^{1}H-NMR (400 MHz, $CDCl_3$, δ): 8.70 (dd, 4H, Ar H), 7.98 (d, 2H, Ar H), 7.82 (dd, 2H, Ar H), 7.71 (d, 2H, Ar H), 7.54 (dd, 4H, Ar H). ^{13}C-NMR (101 MHz, $CDCl_3$, δ): 192.72, 150.38, 146.96, 144.31, 139.55, 135.38, 133.56, 123.10, 121.46, 121.28. MS (ESI+) m/z: [M+H]+ Calcd for C23H14N2O, 334.36; found 335.12. Anal. Calcd for C23H14N2O: C 82.64, H 4.19, N 8.38; O 4.79; found: C 82.80, H 4.18, N 8.40, O 4.63.

Supporting Figures

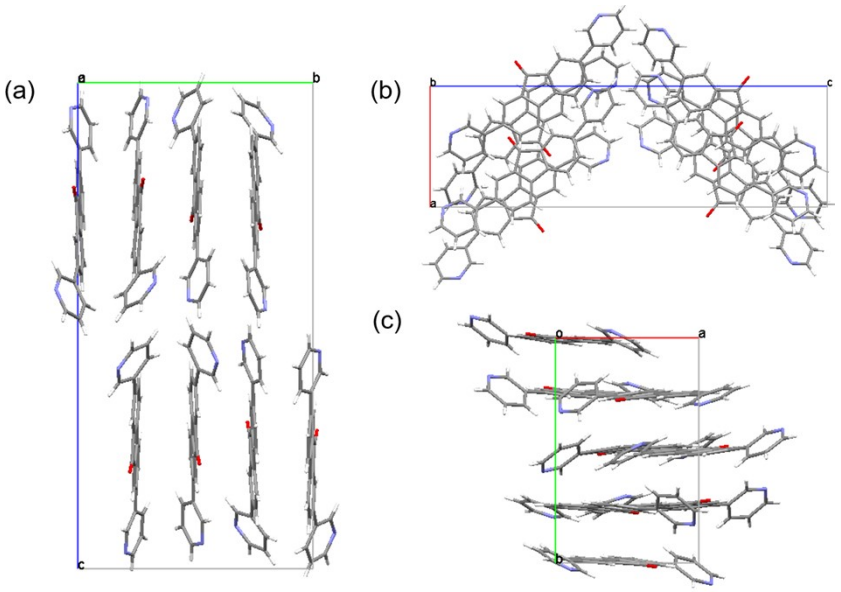

Figure S1. Molecular packing of 3-DPyFO-α in a unit cell along the crystallographic (a) *a*-axis, (b) *b*-axis and (c) *c*-axis, respectively.

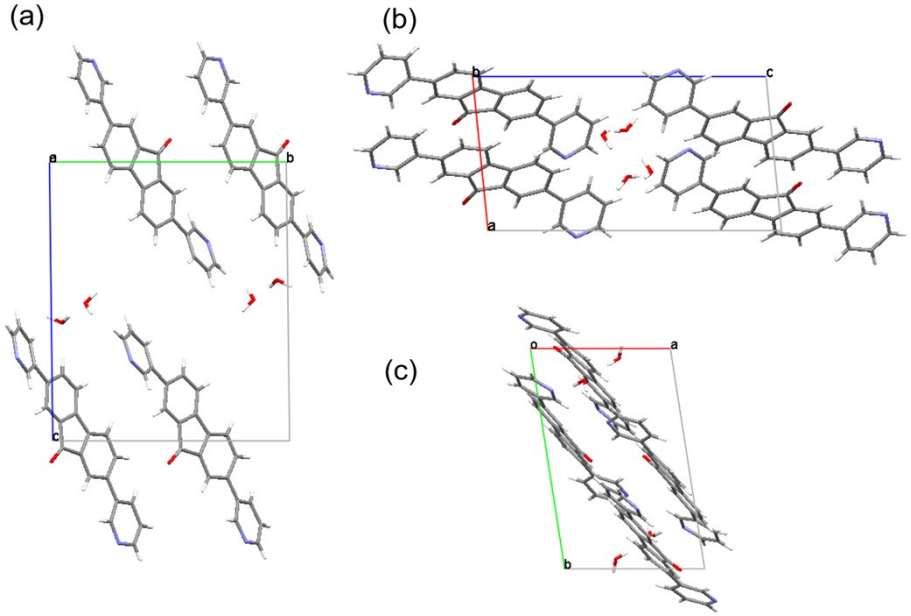

Figure S2. Molecular packing of 3-DPyFO-β in a unit cell along the crystallographic (a) *a*-axis, (b) *b*-axis and (c) *c*-axis, respectively. The disordered solvent molecule (toluene) in the structure is not shown here.

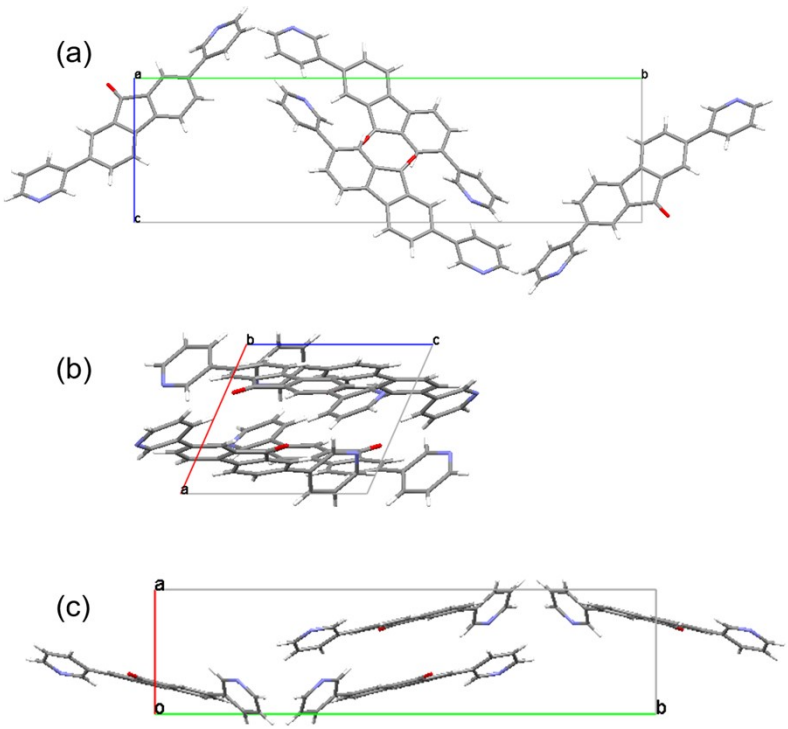

Figure S3. Molecular packing of 3-DPyFO-γ in a unit cell along the crystallographic (a) *a*-axis, (b) *b*-axis and (c) *c*-axis, respectively.

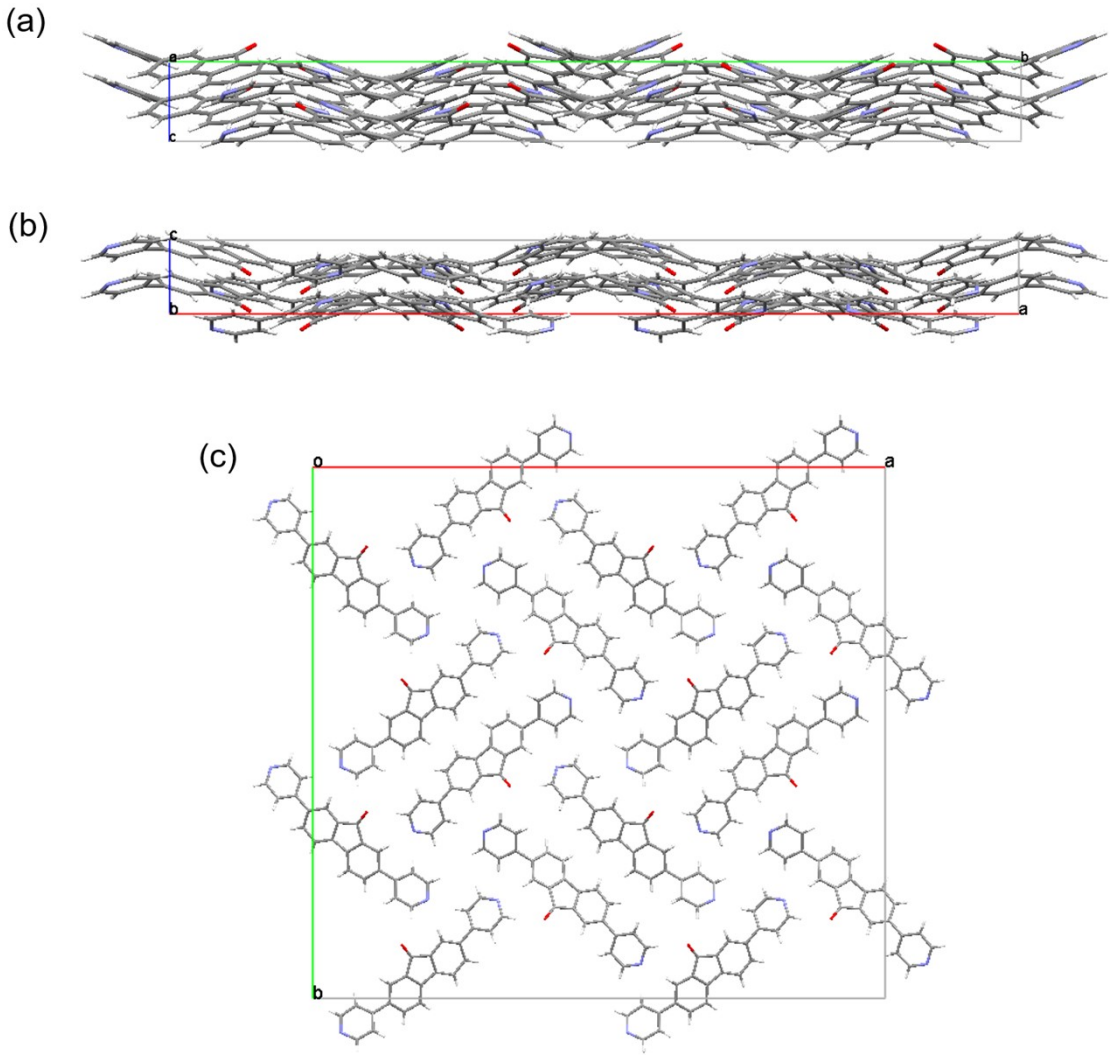

Figure S4. Molecular packing of 4-DPyFO-α in a unit cell along the crystallographic (a) *a*-axis, (b) *b*-axis and (c) *c*-axis, respectively.

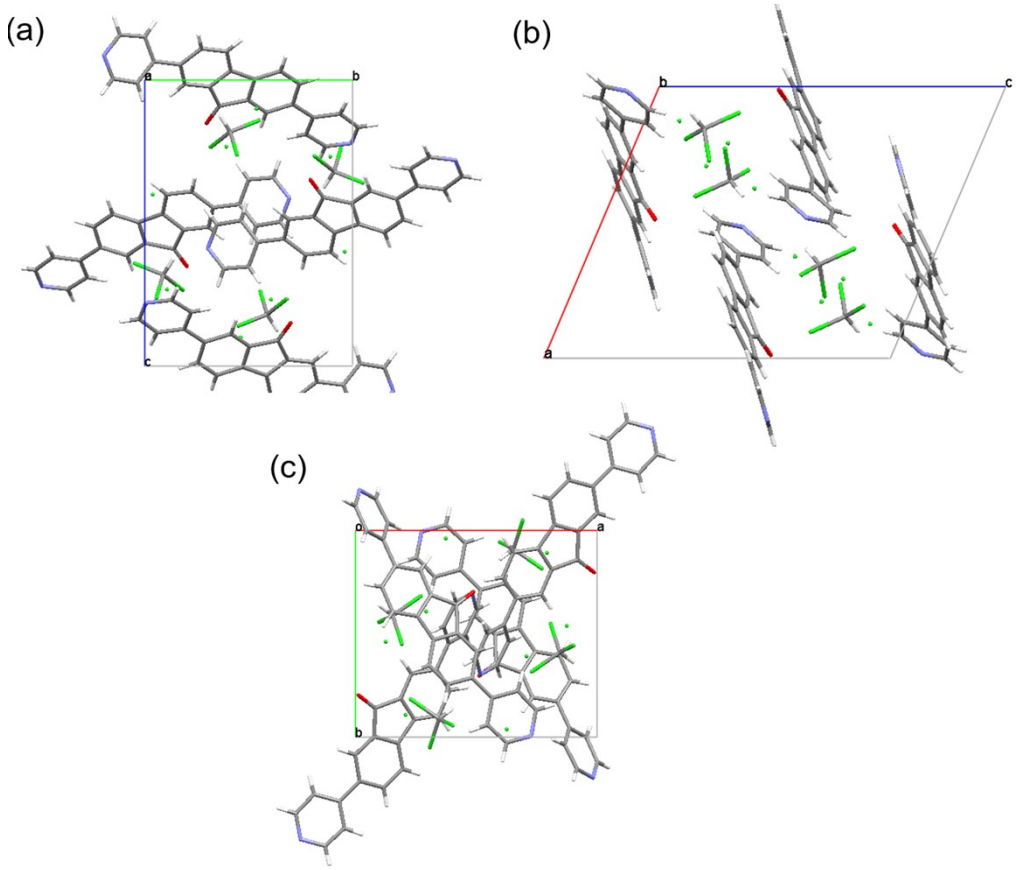

Figure S5. Molecular packing of 4-DPyFO-β in a unit cell along the crystallographic (a) *a*-axis, (b) *b*-axis and (c) *c*-axis, respectively. The shown "non-bond Cl atom" is caused by the disordered solvent (trichloromethane) in the structure.

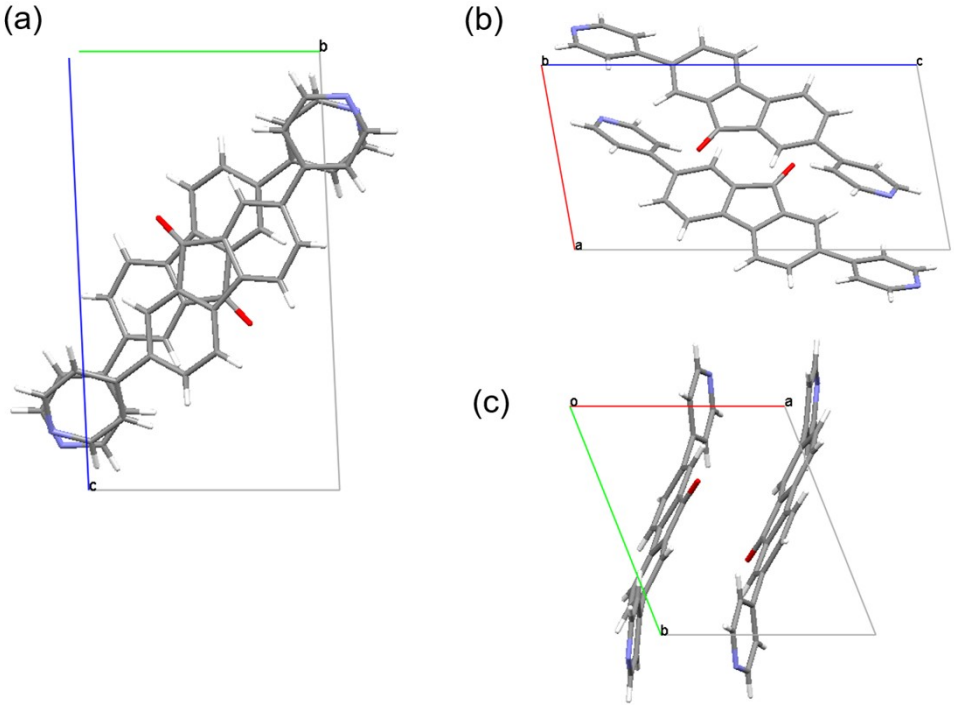

Figure S6. Molecular packing of 4-DPyFO-γ in a unit cell along the crystallographic (a) *a*-axis, (b) *b*-axis and (c) *c*-axis, respectively.

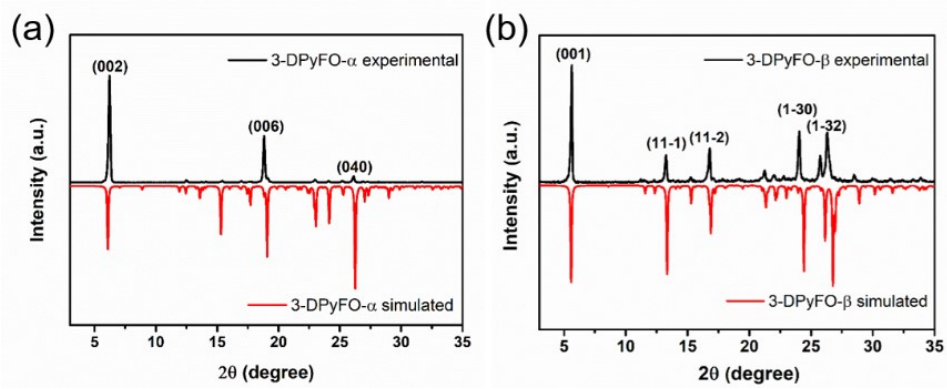

Figure S7. PXRD patterns with face indexation of the as-prepared (a) 3-DPyFO-α and (b) 3-DPyFO-β, in comparison with the simulated patterns. The obtained 4-DPyFO-γ crystals were too few for PXRD measurements.

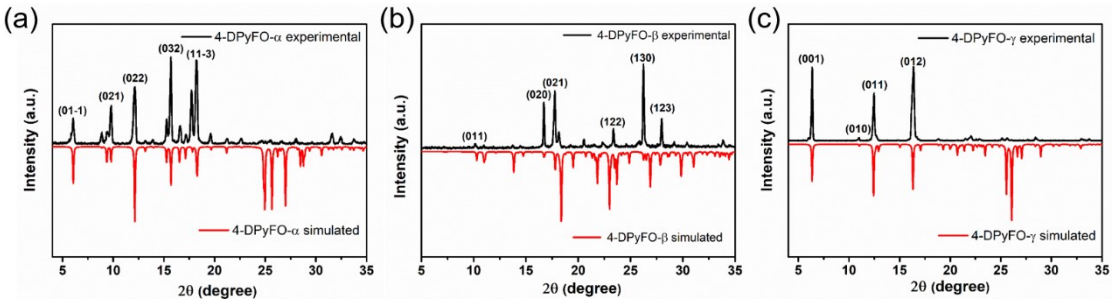

Figure S8. PXRD patterns with face indexation of the as-prepared (a) 4-DPyFO-α, (b) 4-DPyFO-β and (c) 4-DPyFO-γ, in comparison with the simulated patterns.

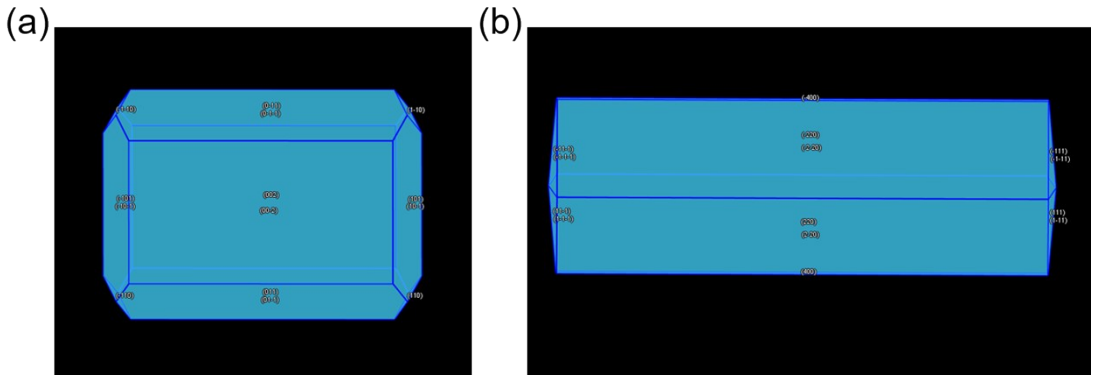

Figure S9. The calculated morphologes with face indexation of (a) 3-DPyFO-α (view along the crystallographic *c*-axis) and (b) 4-DPyFO-α (view along the crystallographic *b*-axis) using the single crystal data and attachment theory.

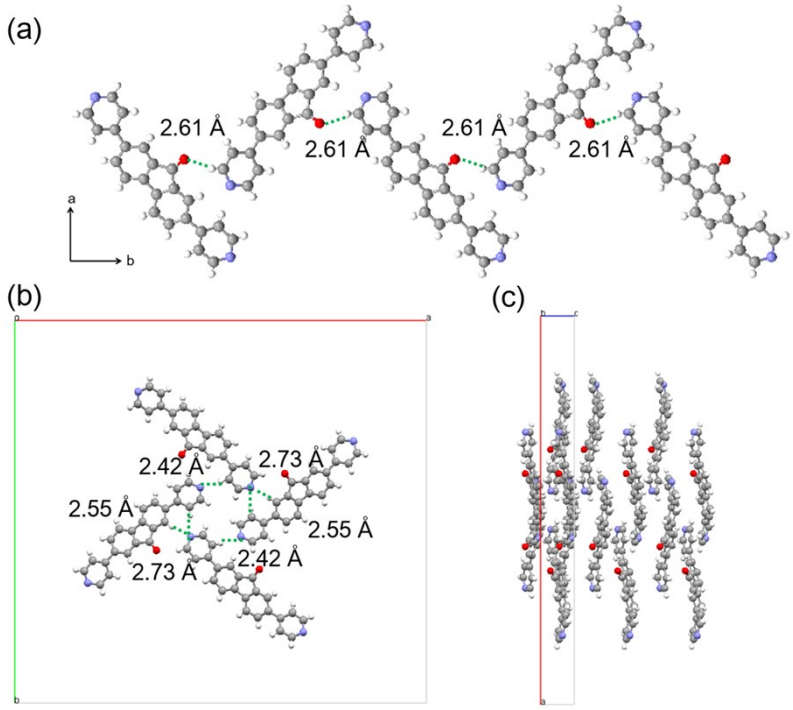

Figure S10. (a) The C=O…H hydrogen bonds driving the molecules to align zig-zag along the crystallographic *b*-axis. (b) Three C-H…N hydrogen bonds of varying strength contribute to the arrangement of the four 4-DPyFO molecules into a paddlewheel shape and (c) stacking along the crystallographic *c*-axis.

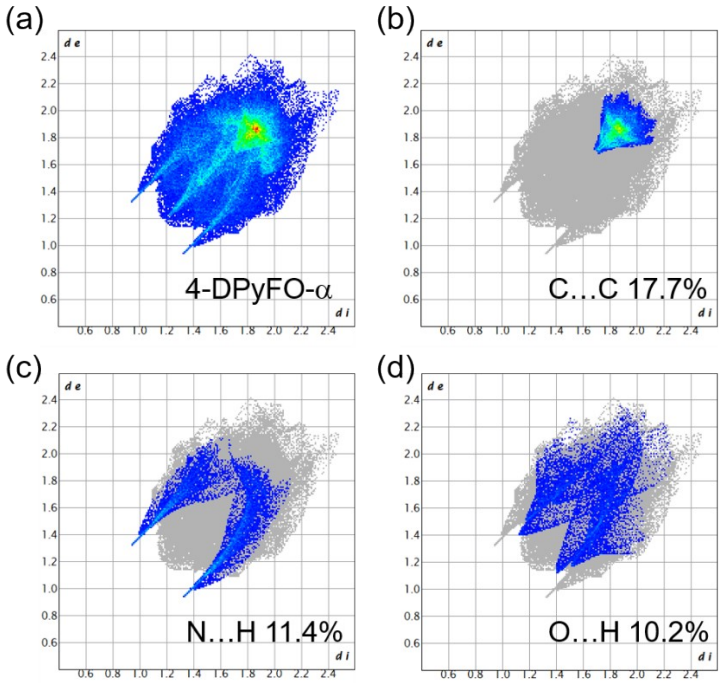

Figure S11. The hirshfeld surfaces and the 2D fingerprint plots of 4-DPyFO-α. (a) Full 2D fingerprint plot of 4-DPyFO-α. (b) C…C interactions fingerprint. (c) N…H interactions fingerprint. (d) O…H interactions fingerprint. The red area means a strong interaction, while the blue area refers to a weak one.

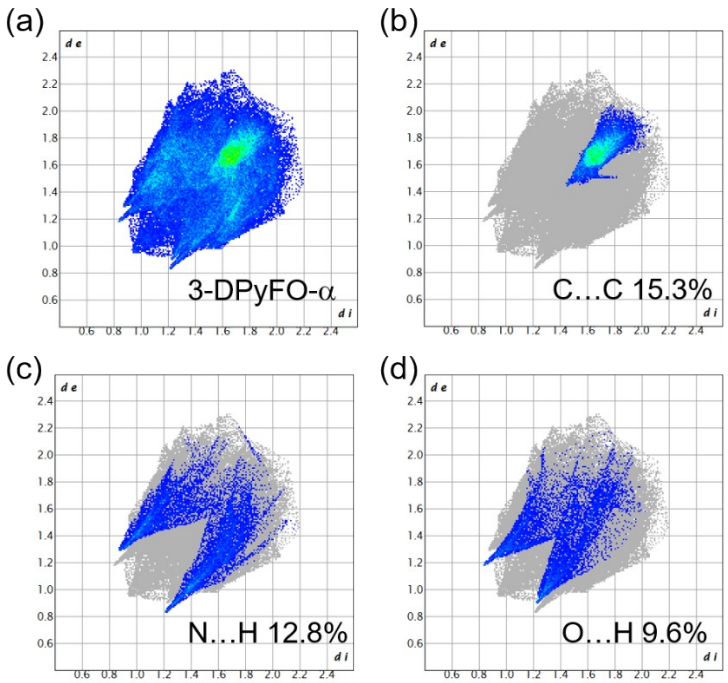

Figure S12. The hirshfeld surfaces and the 2D fingerprint plots of 3-DPyFO-α. (a) Full 2D fingerprint plot of 3-DPyFO-α. (b) C…C interactions fingerprint. (c) N…H interactions fingerprint. (d) O…H interactions fingerprint. The red area means a strong interaction, while the blue area refers to a weak one.

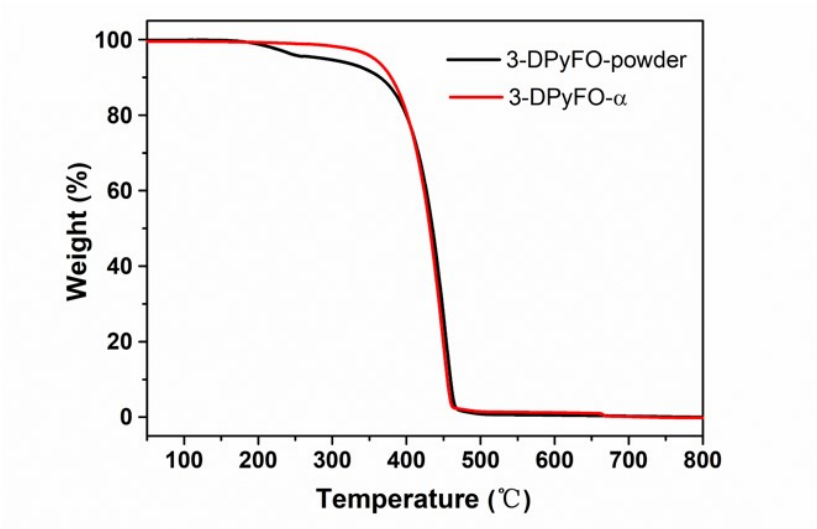

Figure S13. TGA curves of 3-DPyFO powder and 3-DPyFO-α.

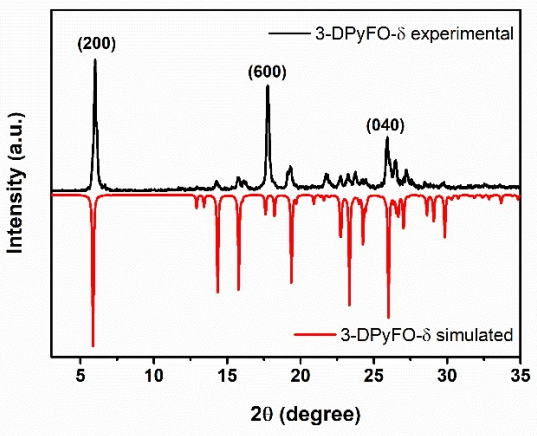

Figure S14. PXRD pattern with face indexation of the 3-DPyFO-δ compared to the simulated patterns.

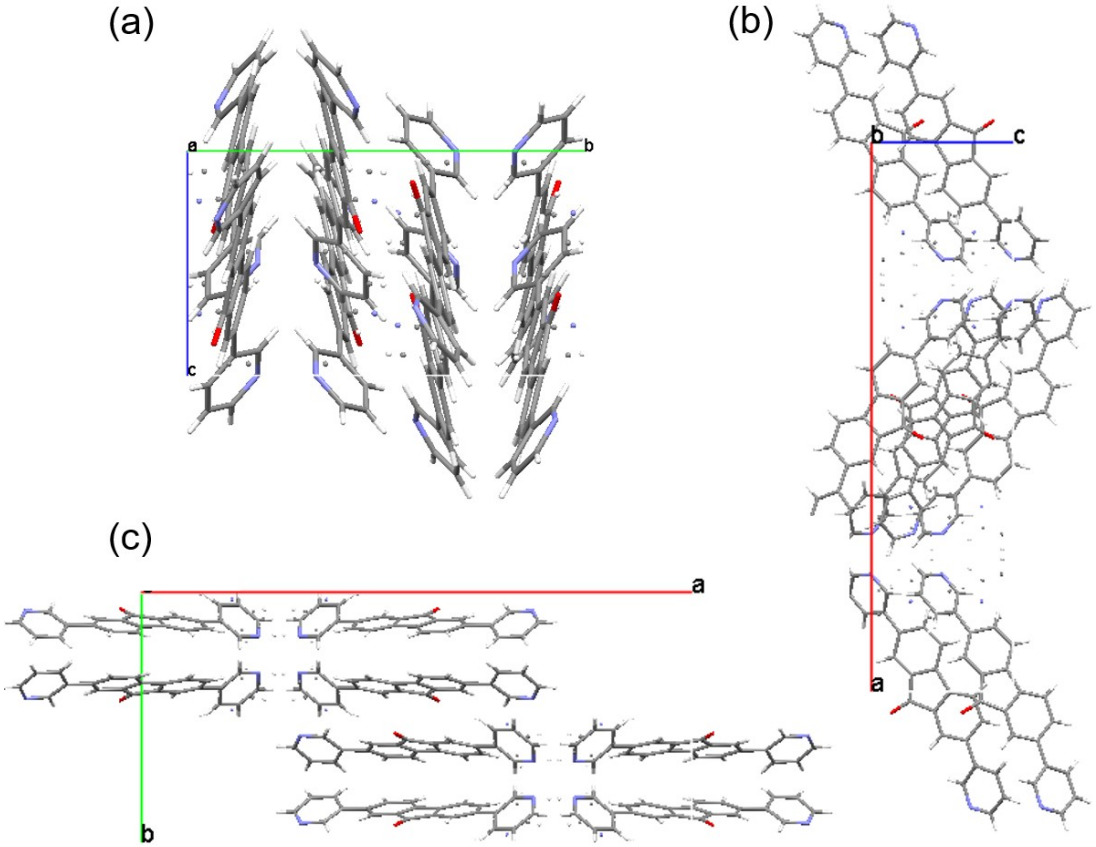

Figure S15. Molecular packing of 3-DPyFO-δ in a unit cell along the crystallographic (a) *a*-axis, (b) *b*-axis and (c) *c*-axis. The shown "non-bond atom" is caused by the disordered pyridine in the molecule.

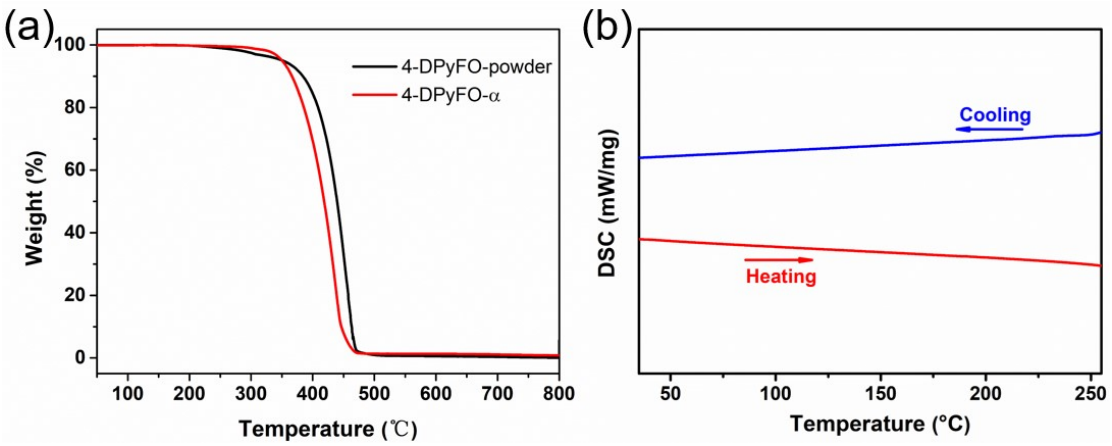

Figure S16. (a) TGA curves of 4-DPyFO powder and 4-DPyFO-α; (b) DCS curves of 4-DPyFO-α.

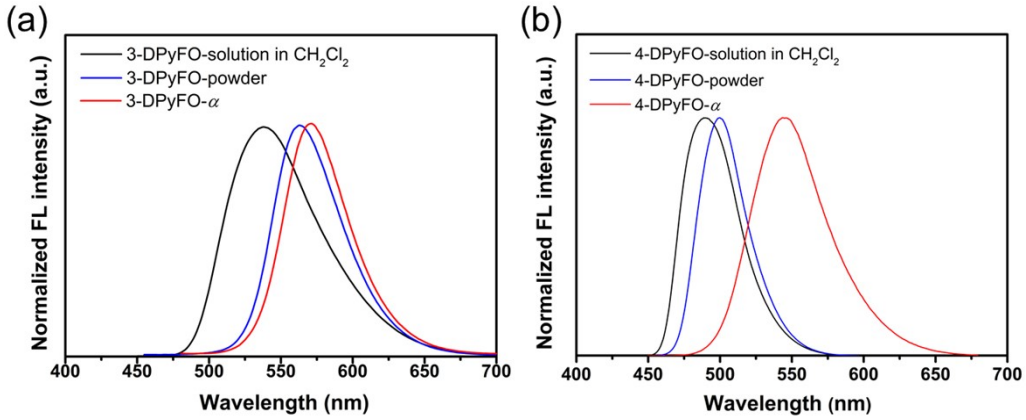

Figure S17. PL spectra of (a) 3-DPyFO and (b) 4-DPyFO. Concentration: 10^{-5} mol L^{-1} in CH_2Cl_2.

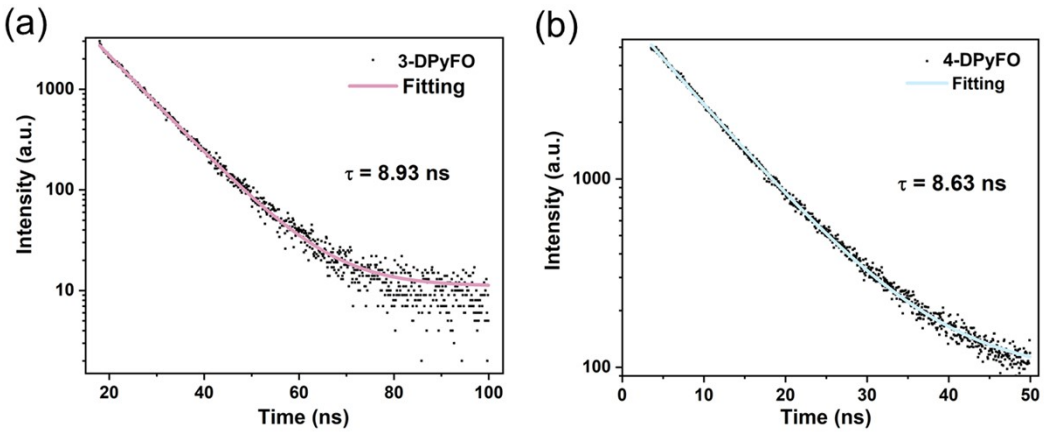

Figure S18. PL decay curves of (a) 3-DPyFO (@582 nm) and (b) 4-DPyFO (@565 nm) powders. The samples were excited by a 365 nm pulsed diode laser at RT.

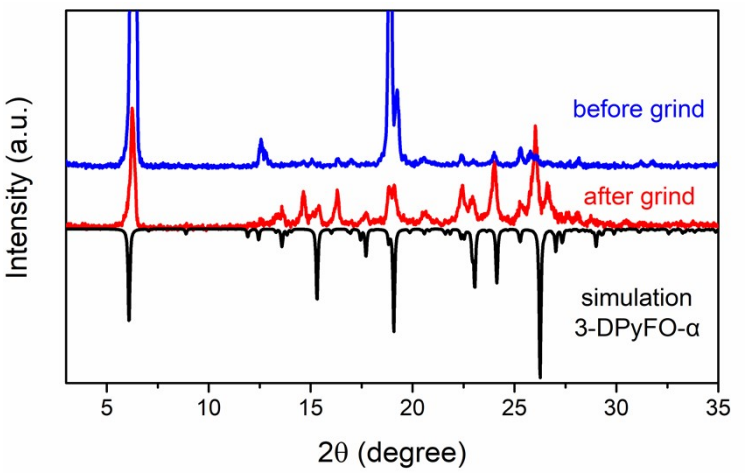

Figure S19. PXRD patterns of 3-DPyFO-α before and after grinding, in comparison with the simulation patterns.

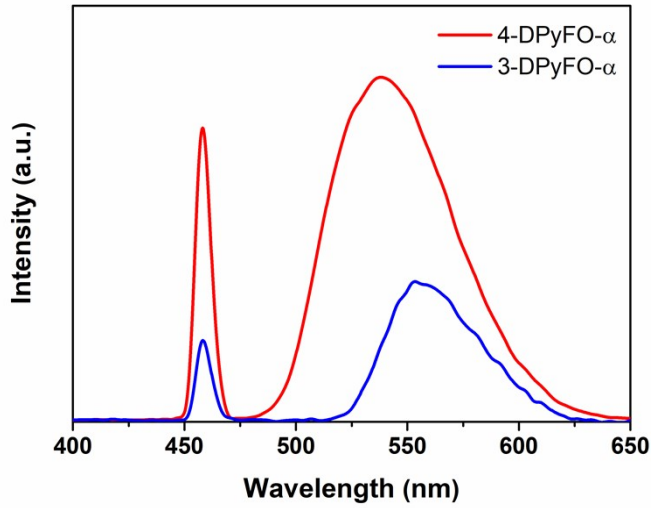

Figure S20. The comparison of SHG intensity between 3-DPyFO-α and 4-DPyFO-α under the same measure conditions. Incident power: 50 mW at 920 nm.

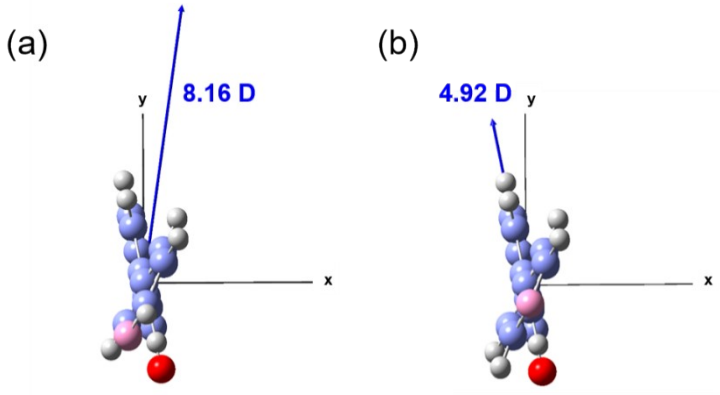

Figure S21. Magnitude and direction of permanent dipole moment of (a) 3-DPyFO and (b) 4-DPyFO molecules.

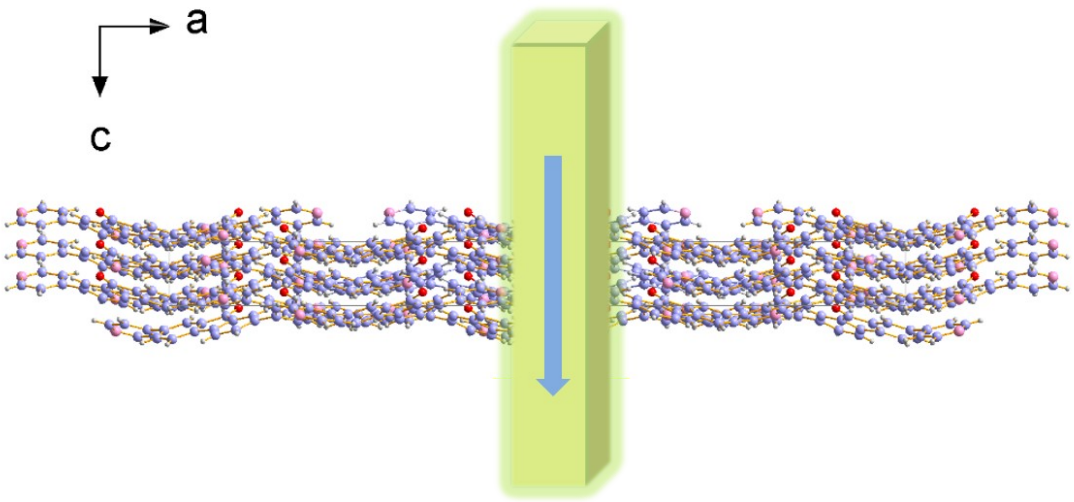

Figure S22. The calculated direction of the overall inherent dipole moment in the cell of 4-DPyFO-α along the crystallographic *c*-axis, in line with the long axis of the microrod crystal. Blue arrow: direction of the overall permanent dipole moment in the unit cell.

Supporting Tables

Table S1. Crystal data and refinement results for 3-DPyFO.

Compound	3-DPyFO-α	3-DPyFO-β	3-DPyFO-γ
Formula	$C_{23}H_{14}N_2O$	$C_{53}H_{40}N_4O_4$	$C_{23}H_{14}N_2O$
CCDC	2106430	2106425	2106424
Formula mass	334.36	755.82	334.36
Temperature (K)	293(2)	99.96(10)	300.78(10)
Crystal system	orthorhombic	triclinic	monoclinic
Space group	$P2_12_12_1$	P-1	$P2_1/c$
a (Å)	8.52570(10)	8.5136(10)	7.5282(2)
b (Å)	13.4455 (2)	13.5667(2)	27.6641(6)
c (Å)	27.9047(4)	15.9278(3)	8.6003(2)
α (°)	90	88.41(10)	90
β (°)	90	84.09(10)	113.78(3)
γ (°)	90	81.09(10)	90
V (Å^3)	3198.78(8)	1807.66(5)	1639.00(8)
Z	8	2	4
D_c (g/cm^3)	1.389	1.389	1.355
μ (mm^{-1})	0.682	0.089	0.665
Final R indexes [I > = 2sigma (I)]	R_1 = 0.0314, wR_2 = 0.0809	R_1 = 0.0544, wR_2 = 0.1539	R_1 = 0.0410, wR_2 = 0.1104
Final R indexes [all data]	R_1 = 0.0339, wR_2 = 0.0827	R_1 = 0.0593, wR_2 = 0.1650	R_1 = 0.0586, wR_2 = 0.1204
F(000)	1392.00	790.00	696.00
Index ranges	-10 ≤ h ≤ 5, -16 ≤ k ≤ 16, -34 ≤ l ≤ 33	-10 ≤ h ≤ 10, -13 ≤ k ≤ 16, -19 ≤ l ≤ 19	-9 ≤ h ≤ 9, -34 ≤ k ≤ 32, -10 ≤ l ≤ 8
GDF on F^2	1.088	1.054	1.056
Reflections collected	15473	18640	8101
Flack	0.16(13)	-	-

Table S2. Crystal data and refinement results for 4-DPyFO.

Compound	4-DPyFO-α	4-DPyFO-β	4-DPyFO-γ
Formula	$C_{23}H_{14}N_2O$	$C_{24}H_{15}Cl_3N_2O$	$C_{23}H_{18}N_2O_3$
CCDC	2106428	2106429	2106427
Formula mass	334.36	453.73	368.38
Temperature (K)	100.02(1)	100.10(1)	293(2)
Crystal system	orthorhombic	monoclinic	triclinic
Space group	*Fdd2*	$P2_1/n$	*P*-1
a (Å)	42.8575(1)	13.4267(4)	7.8189(9)
b (Å)	39.7716(1)	10.5667(3)	8.8169(1)
c (Å)	3.71790(1)	15.7768(5)	14.555(1)
α (°)	90	90	82.99(8)
β (°)	90	113.05(3)	77.87(8)
γ (°)	90	90	67.35(1)
V (Å^3)	6337.2(4)	2059.63(1)	904.37(1)
Z	16	4	2
D_c (g/cm^3)	1.402	1.463	1.353
μ (mm^{-1})	0.688	4.183	0.737
Final *R* indexes [I >= 2sigma (I)]	R_1 = 0.0479, wR_2 = 0.12338	R_1 = 0.0644, wR_2 = 0.1905	R_1 = 0.0913, wR_2 = 0.2522
Final *R* indexes [all data]	R_1 = 0.0494, wR_2 = 0.1353	R_1 = 0.0700, wR_2 = 0.1971	R_1 = 0.1032, wR_2 = 0.2649
F(000)	2784.0	928.0	384.0
Index ranges	-52 ≤ h ≤ 46, -48 ≤ k ≤ 48, -2 ≤ l ≤ 4	-13 ≤ h ≤ 16, -10 ≤ k ≤ 12, -18 ≤ l ≤ 19	-9 ≤ h ≤ 8, -10 ≤ k ≤ 10, -18 ≤ l ≤ 17
GDF on F^2	1.092	1.044	1.093
Reflections collected	15986	10116	7777

Table S3. Crystal data of 3-DPyFO-α and 3-DPyFO-*δ*.

Compound	3-DPyFO-*α*	3-DPyFO-*δ*
Formula	$C_{23}H_{14}N_2O$	$C_{23}H_{14}N_2O$
CCDC	2106430	2106426
Formula mass	334.36	334.36
Temperature (K)	293(2)	100.00(10)
Crystal system	orthorhombic	orthorhombic
Space group	$P2_12_12_1$	*Pccn*
a (Å)	8.52570(10)	30.1793(7)
b (Å)	13.4455 (2)	13.6976(3)
c (Å)	27.9047(4)	7.76620(10)
α (°)	90	90
β (°)	90	90
γ (°)	90	90
V (Å^3)	3198.78(8)	3210.42(1)
Z	8	8
D_c (g/cm^3)	1.389	1.384
μ (mm^{-1})	0.682	0.680
Final *R* indexes [I > = 2sigma (I)]	$R_1 = 0.0314$, $wR_2 = 0.0809$	$R_1 = 0.0579$, $wR_2 = 0.1695$
Final *R* indexes [all data]	$R_1 = 0.0339$, $wR_2 = 0.0827$	$R_1 = 0.0688$, $wR_2 = 0.1795$
F(000)	1392.00	1392.0
Index ranges	$-10 \le h \le 5$, $-16 \le k \le 16$, $-34 \le l \le 33$	$-37 \le h \le 34$, $-11 \le k \le 17$, $-5 \le l \le 9$
GDF on F^2	1.088	1.064
Reflections collected	15473	7980

Supporting References

1. J. Xu, S. Semin, D. Niedzialek, P. H. Kouwer, E. Fron, E. Coutino, M. Savoini, Y. Li, J. Hofkens, I. H. Uji, D. Beljonne, T. Rasing and A. E. Rowan, Self-assembled organic microfibers for nonlinear optics, *Adv. Mater.*, 2013, **25**, 2084-2089.
2. J. P. Perdew, K. Burke and M. Ernzerhof, Generalized Gradient Approximation Made Simple, *Phys. Rev. Lett.*, 1996, **77**, 3865-3868.
3. W. Humphrey, A. Dalke and K. Schulten, VMD: Visual molecular dynamics, *J. Mol. Graphics*, 1996, **14**, 33-38.
4. P. R. Spackman, M. J. Turner, J. J. McKinnon, S. K. Wolff, D. J. Grimwood, D. Jayatilaka and M. A. Spackman, CrystalExplorer: a program for Hirshfeld surface analysis, visualization and quantitative analysis o molecular crystals, *J. Appl. Crystallogr.*, 2021, **54**, 1006-1011.
5. G. Kresse and J. Hafner, Ab initio molecular dynamics for liquid metals, *Phys. Rev. B*, 1993, **47**, 558-561.
6. D. M. E. Freeman, A. J. Musser, J. M. Frost, H. L. Stern, A. K. Forster, K. J. Fallon, A. G. Rapidis, F. Cacialli, I. McCulloch, T. M. Clarke, R. H. Friend and H. Bronstein, Synthesis and Exciton Dynamics of Donor-Orthogonal Acceptor Conjugated Polymers: Reducing the Singlet–Triplet Energy Gap, *J. Am. Chem. Soc.*, 2017, **139**, 11073-11080.